ELSEVIER

Journal of Chromatography A, 890 (2000) 61–72

JOURNAL OF CHROMATOGRAPHY A

www.elsevier.com/locate/chroma

Determination of the intraparticle electroosmotic volumetric flow-rate, velocity and Peclet number in capillary electrochromatography from pore network theory

B.A. Grimes, J.J. Meyers, A.I. Liapis*

Department of Chemical Engineering and Biochemical Processing Institute, University of Missouri-Rolla, Rolla, MO 65409-1230, USA

Abstract

The results obtained from the pore network model employed in this work, clearly show that the magnitudes of the intraparticle electroosmotic volumetric flow-rate, Q_{intrap}, and velocity, $\langle v_{intrap,x} \rangle$, in the pores of the charged porous silica particles considered in this study are greater than zero. The intraparticle Peclet number, Pe_{intra}, of a solute in these charged porous silica particles would be greater than zero, and, in fact, the magnitude of the intraparticle Peclet number, Pe_{intrap}, of lysozyme is greater than unity for all the values of the pore connectivity, n_T, of the intraparticle pores and of the applied electric potential difference per unit length, E_x, along the axis of the capillary column considered in this work. Furthermore, the values of the intraparticle electroosmotic volumetric flow-rate, Q_{intrap}, and velocity, $\langle v_{intrap,x} \rangle$, as well as the magnitude of the pore diffusion coefficient, D_p, of the solute increase as the value of the pore connectivity, n_T, of the intraparticle pores increases. The intraparticle electroosmotic flow can contribute significantly, if the appropriate chemistry is employed in the mobile liquid phase and in the charged porous particles, in (i) decreasing the intraparticle mass transfer resistance, (ii) decreasing the dispersive mass transfer effects, and (iii) increasing the intraparticle mass transfer rates so that high column efficiency and resolution can be obtained.

Keywords: Electrochromatography; Pore network model; Electroosmotic flow; Pore diffusion coefficient; Intraparticle electroosmotic velocity; Intraparticle flow; Peclet number; Mathematical modeling

1. Introduction

In order to design and evaluate properly capillary electrochromatography (CEC) systems, one would have to determine accurately [1,2] the velocity profile of the electroosmotic flow (EOF) in the interstitial channels of bulk flow in packed beds as well as in the intraparticle pores of the porous chromatographic particles used in CEC. Liapis and Grimes [1] constructed and solved a mathematical model to describe quantitatively the profiles of the electrostatic potential, pressure, and velocity of the EOF in charged cylindrical capillaries and in CEC systems. They compared [1] their theoretical results for the velocity of the EOF with the experimental values of the velocity of the EOF obtained from a fused-silica column packed with charged porous silica C_8 particles; systems with four different particle diameters ($d_p = 0.2$ μm; $d_p = 0.5$ μm; $d_p = 1.0$ μm; and $d_p = 3.0$ μm) and three different electrolyte concentrations ($C_\infty = 5.0$ mM; $C_\infty = 10.0$ mM; and $C_\infty = 25.0$ mM) were considered and the magnitude of the applied electric potential difference per unit length, E_x, was varied widely (10 kV/m $\leq E_x \leq$ 80 kV/m). The agreement between the theoretical re-

*Corresponding author. Tel.: +1-573-3414-416; fax: +1-573-3412-071.

0021-9673/00/$ – see front matter
PII: S0021-9673(00)00130-8

sults and the experimental data was found [1] to be good. Also, the results from model simulations [1] indicated the conditions which permit high values for the average velocity of the EOF to be obtained, for a given operationally permissible value of the applied electric potential difference per unit length, E_x. Furthermore, model simulations showed [1] that the magnitude of the average velocity of the EOF in the pores of the charged porous particles can be greater than zero; this result indicates that the intraparticle volumetric flow-rate, Q_{intrap}, of the EOF can be greater than zero. It is very important to be able to determine the magnitudes of the intraparticle volumetric flow-rate and velocity of the EOF in the charged porous particles employed in CEC systems, because this intraparticle convective mass transfer mechanism can influence significantly [1], if the appropriate chemistry is employed in the mobile liquid phase and in the charged porous particles, the intraparticle mass transfer resistance and mass transfer rate, as well as the magnitude of the dispersive mass transfer effects.

In this work, the pore network theory of Meyers and Liapis [3,4] and Liapis et al. [5] and the mathematical model for capillary electrochromatography constructed and solved by Liapis and Grimes [1], are employed together in order to estimate the magnitudes of the intraparticle electroosmotic volumetric flow-rate, Q_{intrap}, and velocity, $\langle v_{\text{intrap},x} \rangle$, in the pores of the charged porous silica particles, as well as the magnitude of the intraparticle Peclet number, $\text{Pe}_{\text{intrap}}$, of lysozyme.

2. System formulation

The capillary column packed with charged porous silica particles is topologically mapped onto a cubic lattice network of interconnected cylindrical pores [3–5] and the lattice employed in our work has a regular array of nodes (the lattice size, L, is the same along the x, y and z space coordinates of the network, and thus, $x \times y \times z$: $L \times L \times L$) that are connected to each other by bonds (pores) of the network. The porous structure in the capillary column has (a) interstitial pores which represent the pores between the packed-in-the-capillary column particles and provide the flow channels for bulk electroosmotic flow in the capillary column, and (b) intraparticle pores which represent the pores within the charged porous silica particles; in Fig. 1, a section of a capillary column packed with charged porous particles is presented, as well as a section of a monolith whose pores have charged surfaces. Meyers and Liapis [3,4] and Liapis et al. [5] constructed a pore network modeling theory that can be used to describe and determine quantitatively the convective flow of a solute in the interstitial channels for bulk flow of a packed column (or monolith) and in the pores of the porous particles (or in the pores of the skeletons of a monolith) as well as to determine the value of the pore diffusion coefficient of the solute in the porous particles (or in the pores of the skeletons of a monolith), under retained and unretained conditions. The pore connectivity, n_T, is defined [3–5] as the number of bonds (pores) connected to a single node of the lattice. In this work, the nodes of the cubic lattice are considered to have no volume in the network while the bonds (pores) of the network are considered to provide the pore volume of the network (bond percolation). For mediums whose structure is made from fibers, it could be possible to consider that all the volume of the network is contained in the nodes (sites) and the bonds of the network have no volume (site percolation). The physical information (experimental data) and mathematical expressions and procedure required for the construction of the pore network model are presented in Meyers and Liapis [3,4] and Liapis et al. [5].

In the works of Meyers and Liapis [3,4] and Liapis et al. [5] high-performance liquid chromatography (HPLC) has been considered, and thus, the convective flow of a solute in the interstitial channels for bulk flow and in the intraparticle pores occurs because of the application of a hydrostatic pressure across the length of the column or of the monolith. In CEC, the convective flow of a solute in the interstitial channels for bulk flow and in the intraparticle pores is due to the EOF and occurs because of the application of a potential difference (an electric field) across the length of the column or of the monolith; this electrical potential difference per unit length is denoted by E_x and is applied along the axial direction, x, of the column or of the monolith [1]. The interstitial and intraparticle pores (bonds) of the pore network model constructed and

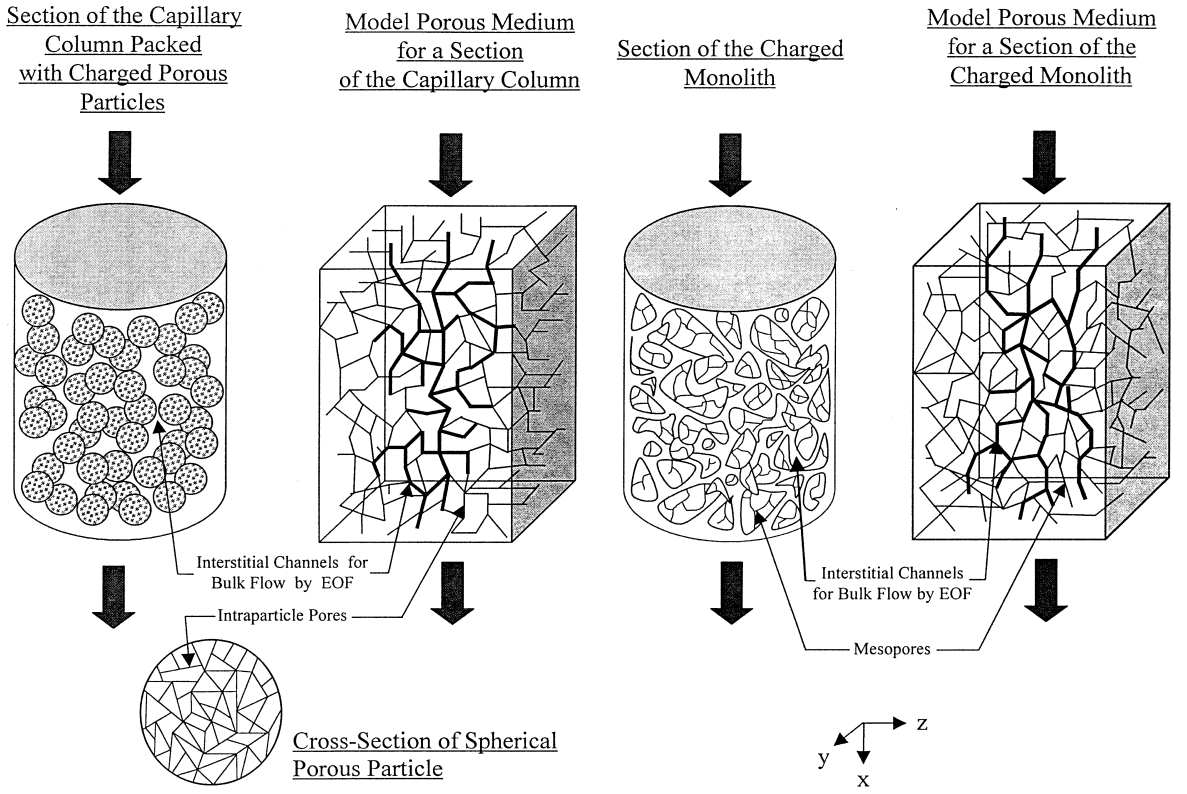

Fig. 1. Schematic representation through the pore network model of a finite small section of a capillary column packed with charged porous particles and of a monolith (continuous bed) whose pores have charged surfaces.

employed for CEC in this work, by utilizing the pore network modeling theory in Refs. [3–5], have directions that are parallel to the axial direction, x, of the capillary column and directions that form an angle θ ($0<\theta\leq\pi/2$) with the axial direction x. The electric potential difference per unit length is E_x for the interstitial and intraparticle pores whose direction is parallel to the axial direction, x, of the capillary column, while for the interstitial and intraparticle pores whose directions form an angle θ with the axial direction, x, the electric potential difference per unit length is $E_x\cos\theta$. The velocity distribution of the EOF along the radius of the pores and the average velocity of the EOF in the pores along the axial direction, x, of the capillary column are determined, for a given value of E_x, from the solution for each pore radius, R_{pore}, of the mathematical model for EOF constructed by Liapis and Grimes [1]. The zeta potential, ζ_p, at the surface of the charged porous particles can be measured experimentally [1,2,7,8], and the value of ζ_p is then used in the expressions in Ref. [1] to determine the fixed charged density, δ, at the surface of the charged porous particles and at the surface of the interstitial and intraparticle pores [1]; then, by employing the value of δ in Eq. (19a) of Ref. [1], the boundary condition of the Poisson–Boltzmann expression (Eq. (15) in Ref. [1]) at the wall of each pore of the pore network model is established. Thus, by using the mathematical model for EOF presented in Ref. [1], the average velocity of the EOF for a given value of E_x is determined in each interstitial and intraparticle pore (located in each layer of the cubic lattice network) that allows net conduction of fluid flow along the axial direction, x, of the capillary column. Then by determining the cross-sectional area for each of these interstitial and intraparticle pores in each layer of the pore network model, the volumetric

flow-rate due to the EOF is calculated in each of these pores through the product of the average velocity of the EOF in each pore with its cross-sectional area. The total amount of the electroosmotic volumetric flow-rate, Q_{inters}, through the interstitial pores is determined (for each layer of the pore network model) by adding the volumetric electroosmotic flow-rates of the interstitial pores (in each layer of the cubic lattice network) that allow net conduction of fluid flow along the axial direction, x, of the capillary column. In a similar way, the total amount of the electroosmotic volumetric flow-rate, Q_{intrap}, through the intraparticle pores is determined (for each layer of the pore network model) by adding the electroosmotic volumetric flow-rates of the intraparticle pores (in each layer of the pore network model) that allow net conduction of fluid flow along the axial direction, x, of the capillary column. The total electroosmotic volumetric flow-rate, Q_{total}, through the capillary column is determined from the sum of Q_{inters} and Q_{intrap}.

The value of the pore diffusion coefficient, D_p, of the solute in the pores (intraparticle pores) of the charged porous particles is determined from the mathematical expressions and procedure presented in the pore network modeling theory developed by Meyers and Liapis [3,4] and Liapis et al. [5].

3. Results and discussion

The radius, r_p, of the charged porous silica particles considered in this work is taken to be equal to 1.5 μm, the bed porosity, ϵ_b, in the fused-silica capillary column of radius $R=50$ μm is 0.35, the porosity, ϵ_p, of the silica particles is 0.49, and the radius R_{ic} of all the interstitial channels (interstitial pores of the pore network model) for bulk flow by EOF in the fused-silica capillary column is considered to be equal to 1/3 of the particle radius, for the reasons discussed in Ref. [1], and thus, $R_{ic}=(1/3)r_p=0.5$ μm; furthermore, the interstitial channels are taken to be parallel with each other. One could consider a different pore size distribution function and pore connectivity for the interstitial pores [3,4], but the purpose of the current study is to examine, through the employment of pore network theory [3–5], whether there is a non-zero electroosmotic volumetric flow-rate, Q_{intrap}, and velocity, $\langle v_{intrap,x}\rangle$, in the intraparticle pores (in the pores of the charged porous silica particles) for a given pore size distribution function and pore connectivity, n_T, of the intraparticle pores; the pore network theory in Refs. [3,4] could consider any physically appropriate pore connectivity value and functional form of the pore size distribution of the interstitial pores for bulk flow (by EOF) in the fused-silica capillary column. The functional form of the pore size distribution of the pores in the charged porous silica particles considered in this work is given by Eq. (1):

$$f(d_{intrap}) = \left(\frac{1}{\sqrt{2\pi\sigma}}\right) \times \left\{\exp\left[-\frac{1}{2}\cdot\left(\frac{d_{intrap}-\mu}{\sigma}\right)^2\right]\right\} \quad (1)$$

which represents a Gaussian distribution. In Eq. (1), d_{intrap} denotes the diameter of the intraparticle pores, μ represents the mean diameter of the intraparticle pores, and σ is the standard deviation of the diameter of the intraparticle pores. The value of the mean diameter, μ, of the pores in the charged silica particles considered in this work is 115.1 Å, while the value of the standard deviation, σ, is 30.2 Å. For all the simulations presented in this work, a lattice size of $10\times10\times10$ was used for the cubic lattice because it could provide a reasonable representation of the pore network model and does not require excessive computational times [3,4]. Furthermore, pore network models with coordination numbers six and 18 [6] were considered. The value of the intraparticle pore connectivity, n_T, was varied between two and six for the pore network model whose coordination number [3–6] is six, while the value of n_T was varied between two and 18 for the pore network model whose coordination number is 18.

The liquid phase in the interstitial and intraparticle pores is acetonitrile–25 m*M* Tris–HCl (80:20) at pH 8.0 and temperature $T=20$°C, the solute is lysozyme, and the CEC system operates under unretained conditions [1]. This electrolyte is symmetric, the value of the dielectric constant, ϵ, is equal to 47.8 $esu^2\ dyne^{-1}\ cm^{-2}$ ($4.2288\cdot10^{-10}\ C^2\ N^{-1}\ m^{-2}$), the value of the Debye length, λ, that represents the characteristic length of the double layer is equal to 14.88 Å [1], and the values of the density and

viscosity of the liquid phase are 836.77 kg/m^3 and $4.99 \cdot 10^{-4}$ kg m^{-1} s^{-1}, respectively. The zeta potential, ζ_p, at the surface of the charged porous silica particles is -64.1 mV [1], and the value of the fixed charge density, δ, at the surface of the charged porous silica particles and at the surface of the interstitial and intraparticle pores is equal [1] to -7004.94 esu/cm^2. The value of the applied electric potential difference per unit length, E_x, along the axial direction, x, of the capillary column is varied, in this work, from 20 kV/m to 100 kV/m.

In Fig. 2, the percentages of the intraparticle electroosmotic volumetric flow-rate, Q_{intrap}, and of the interstitial electroosmotic volumetric flow-rate, Q_{inters}, with respect to the total electroosmotic volumetric flow-rate, Q_{total}, in the capillary column versus the intraparticle pore connectivity, n_T, are presented, when the coordination number of the pore network is six (Fig. 2a) and when the coordination number of the pore network is 18 (Fig. 2b). The values of the ratios Q_{intrap}/Q_{total} and Q_{inters}/Q_{total} are the same for all values of E_x because, for a given packed capillary column, these ratios are determined from the interstitial and intraparticle pore structures [3–5] of the given packed capillary column; as the value of E_x increases, the values of Q_{intrap}, Q_{inters}, and Q_{total} increase but the values of the ratios Q_{intrap}/Q_{total} and Q_{inters}/Q_{total} remain unchanged. The results in Fig. 2 indicate that the ratio Q_{intrap}/Q_{total} increases as the value of the intraparticle pore connectivity, n_T, increases, while the ratio Q_{inters}/Q_{total} decreases with increasing values of the intraparticle pore connectivity, n_T. Furthermore, the results in Fig. 2 show that the value of Q_{intrap}, for the values of the intraparticle pore connectivity, n_T, and charged porous silica particles considered in this work, is between 0.09% and 5.20% of the value of Q_{total}, and therefore, 94.80% to 99.91% of the total electroosmotic volumetric flow-rate, Q_{total}, occurs in the interstitial channels (pores) for bulk flow of the packed capillary column. Although the magnitude of Q_{intrap} in Fig. 2 is only between 0.09% and 5.20% of the value of Q_{total}, the impact of this intraparticle convective mass transfer mechanism on reducing the intraparticle mass transfer resistance could be significant, if the appropriate chemistry is employed in the mobile liquid phase and in the charged porous particles [9–12].

In Fig. 3, the intraparticle electroosmotic velocity, $\langle v_{intrap,x} \rangle$, along the axial direction, x, of the packed capillary column versus the intraparticle pore connectivity, n_T, is presented, for different values of E_x. The value of $\langle v_{intrap,x} \rangle$ is obtained from the ratio Q_{intrap}/A_{cs} where A_{cs} represents the cross-sectional area of the porous medium (porous particle) that is normal to the axial direction, x, and thus, the intraparticle electroosmotic velocity $\langle v_{intrap,x} \rangle$ represents the superficial velocity of the intraparticle EOF. The results in Fig. 3 indicate that the magnitude of $\langle v_{intrap,x} \rangle$ increases as the value of the intraparticle pore connectivity, n_T, and the magnitude of the applied electric potential difference per unit length, E_x, increase. It can also be observed that the effect of n_T on $\langle v_{intrap,x} \rangle$ becomes more pronounced as the value of E_x increases. Furthermore, the results in Fig. 3 indicate that the magnitude of the intraparticle electroosmotic velocity in the porous silica particles could be significant, if the appropriate chemistry is employed in the mobile liquid phase and in the charged porous particles [9–12], and thus, the intraparticle mass transfer rate due to the intraparticle electroosmotic convective flow can contribute substantially towards the reduction of the intraparticle mass transfer resistance.

In Fig. 4, the ratio of the pore diffusion coefficient, D_p, of lysozyme to the product of ϵ_p with D_{mf} versus the intraparticle pore connectivity, n_T, is presented. The values of the effective molecular radius, α_1, and of the free molecular diffusion coefficient, D_{mf}, of lysozyme are 21.4 Å and $1.006 \cdot 10^{-10}$ m^2/s [3,4,13]. The results in Fig. 4 clearly show that as the intraparticle pore connectivity, n_T, increases, the value of the ratio $D_p/\epsilon_p D_{mf}$ increases. It can be observed that the increase in the value of the ratio $D_p/\epsilon_p D_{mf}$ is small when the range of values of n_T is between 2.0 to 3.5, while for values of n_T in the range of 3.5 to 4.5 the change in the value of the ratio $D_p/\epsilon_p D_{mf}$ is very large; for values of n_T greater than 4.5, the value of the ratio $D_p/\epsilon_p D_{mf}$ increases linearly with a moderate slope. These results are due to the fact that (i) for values of the pore connectivity, n_T, less than 3.5, there are few pores in the cubic lattice of the pore network model that allow net mass transfer of solute by pore diffusion along the axial direction, x, of the porous medium, (ii) for values of the pore connectivity, n_T, in the range of 3.5 to 4.5,

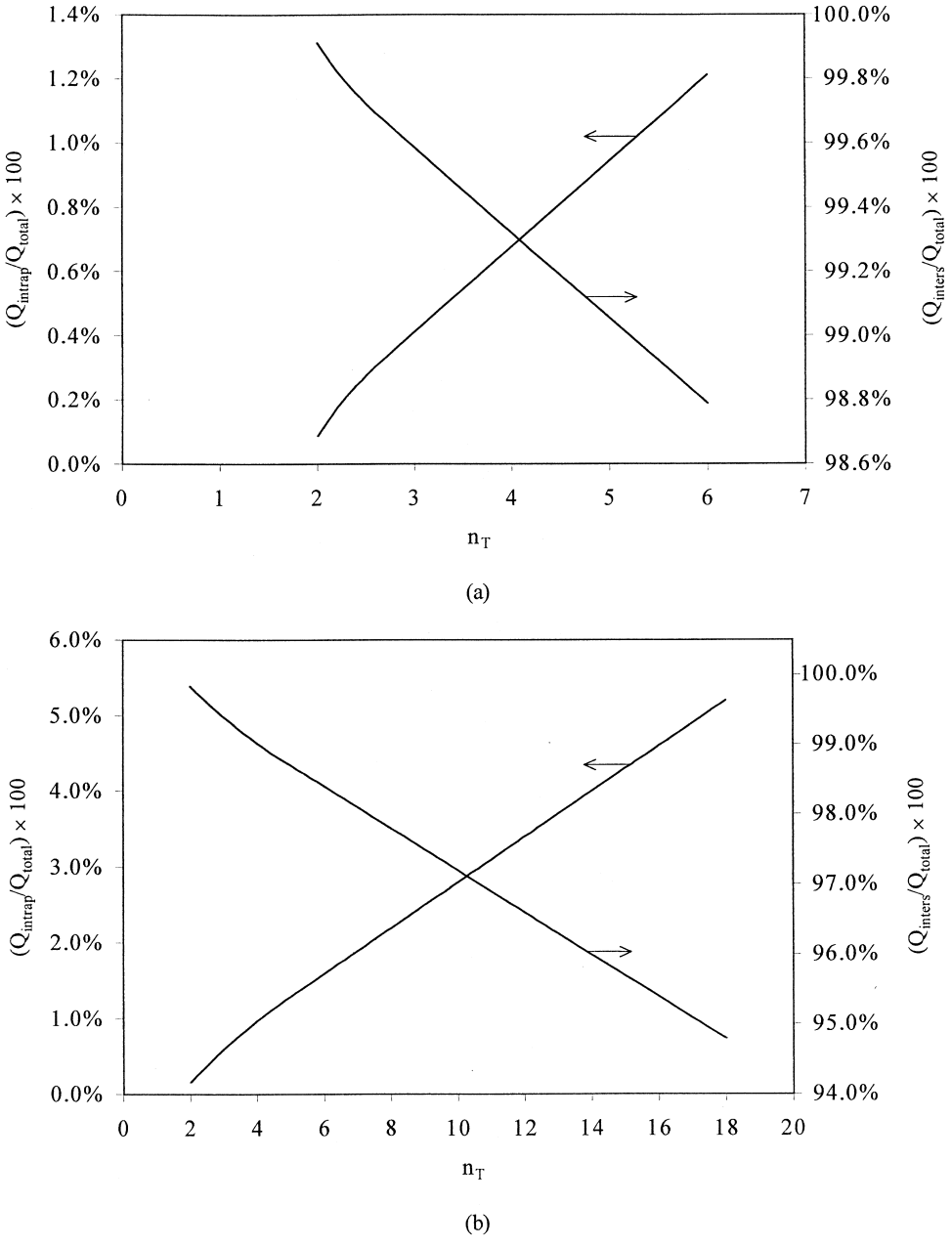

Fig. 2. Percentages of the intraparticle electroosmotic volumetric flow-rate, Q_{intrap}, and of the interstitial electroosmotic volumetric flow-rate, Q_{inters}, with respect to the total electroosmotic volumetric flow-rate, Q_{total}, in the capillary column versus the intraparticle pore connectivity, n_T. (a) Pore network model whose coordination number is equal to six. (b) Pore network model whose coordination number is equal to 18.

there is a substantial number of pores in the cubic lattice of the pore network model that allow net mass transfer of solute by pore diffusion along the axial direction, x, of the porous medium, and (iii) the pore network is highly connected when $n_T = 4.5$, so that the addition of pores to the network as the value of

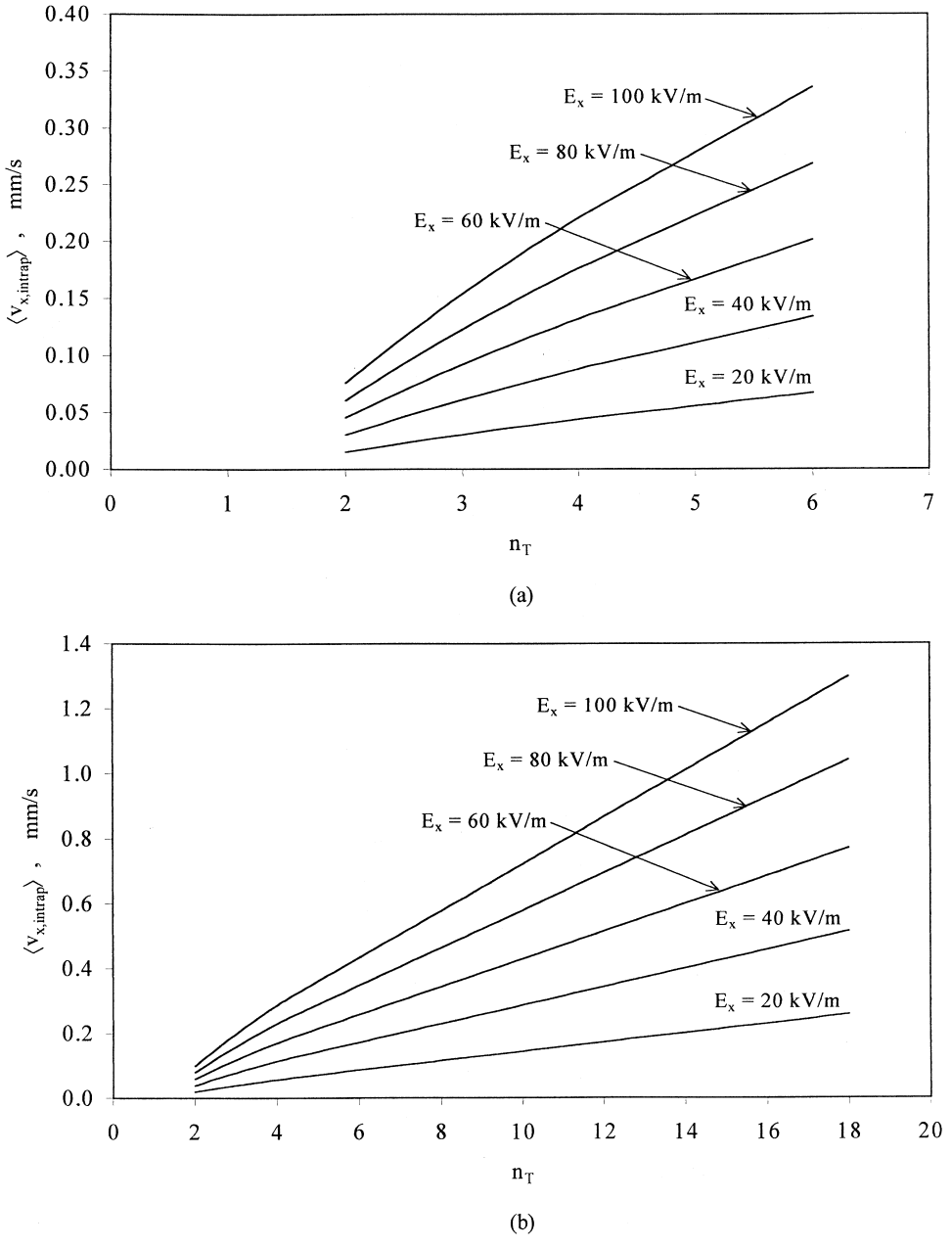

Fig. 3. Superficial intraparticle velocity, $\langle v_{intrap,x} \rangle$, of the electroosmotic flow along the axial direction, x, of the capillary column versus the intraparticle pore connectivity, n_T, for different values of the applied electric potential difference per unit length, E_x. (a) Pore network model whose coordination number is equal to six. (b) Pore network model whose coordination number is equal to 18.

the pore connectivity, n_T, increases above 4.5, does not affect the net mass transfer of solute by pore diffusion along the axial direction, x, of the porous medium as significantly as was the case when the value of n_T was in the range of 3.5 to 4.5. The data in Fig. 4 indicate that the pore network model could allow one to determine, for a given porous medium and for a given solute of interest, the pore diffusion

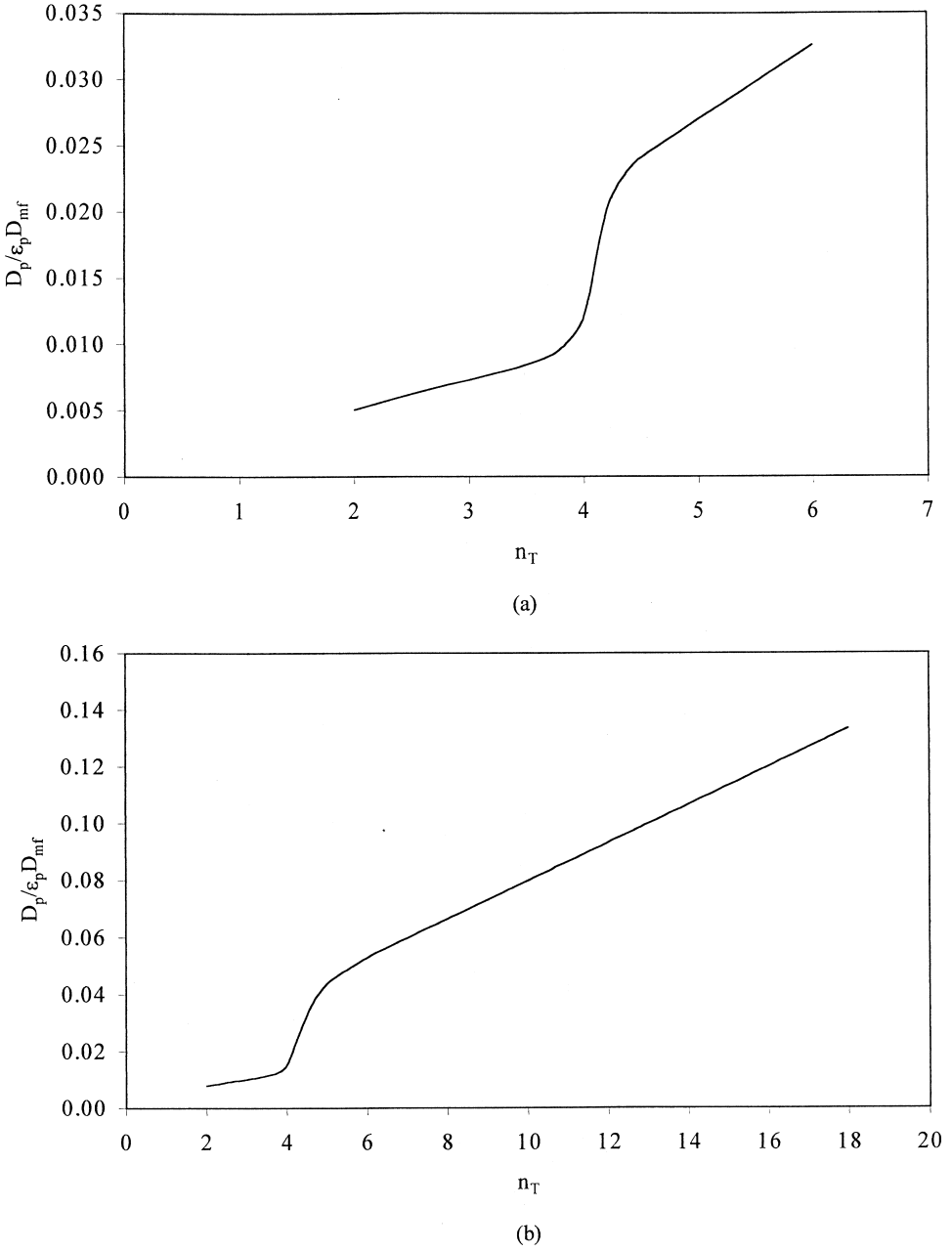

Fig. 4. Ratio of the pore diffusion coefficient, D_p, of lysozyme to $\epsilon_p D_{mf}$ versus the intraparticle pore connectivity, n_T. (a) Pore network model whose coordination number is equal to six. (b) Pore network model whose coordination number is equal to 18.

coefficient, D_p, of the solute in an a priori manner. One does not need to estimate values for the empirical parameter of tortuosity since tortuous pathways for mass transfer are already built within the pore network model. Furthermore, the pore network model properly accounts for the overall restriction to diffusion (overall hindrance) due to steric hindrance at the entrance to the pores and

frictional resistance within the pores [3,4]. If one would consider the empirical relationship $D_p = (\epsilon_p D_{mf})(\beta/\tau)$, where β represents the hindrance parameter of the porous medium and τ denotes the average tortuosity in the porous medium, then the ratio $D_p/\epsilon_p D_{mf}$ in Fig. 4 might be thought of as providing the value of the ratio β/τ in an a priori manner. The results in Fig. 4 indicate that the pore network model can be used to provide in an a priori manner numerical values for the pore diffusion coefficient, D_p, which could then be employed in the macroscopic models that could describe the dynamic behavior of chromatographic separations in columns packed with porous particles [5]. Furthermore, the results in Figs. 2–4 clearly show that charged porous particles whose intraparticle pore structure is described by a pore network model whose coordination number is greater than six, could provide larger values for the intraparticle electroosmotic volumetric flow-rate, Q_{intrap}, the intraparticle electroosmotic velocity, $\langle v_{intrap,x} \rangle$, and for the pore diffusion coefficient, D_p, of the solute.

In Fig. 5, the intraparticle Peclet number, Pe_{intrap}, versus the intraparticle pore connectivity, n_T, is presented for different values of the applied electric potential difference per unit length, E_x, when the coordination number of the pore network model is six (Fig. 5a) and when the coordination number of the pore network model is 18 (Fig. 5b). The intraparticle Peclet number, Pe_{intrap}, represents the ratio of the diffusional response time, t_d, to the convective (EOF) response time, t_c, of a solute in a porous particle, and thus:

$$Pe_{intrap} = \frac{t_d}{t_c} \tag{2}$$

Liapis and Grimes [1] have shown that Pe_{intrap} could be determined from Eq. (3):

$$Pe_{intrap} = \frac{d_p \left\langle v_{intrap,x} \right\rangle}{12 D_p} \tag{3}$$

where d_p denotes the particle diameter ($d_p = 2r_p$) and $\langle v_{intrap,x} \rangle$ represents the intraparticle superficial electroosmotic velocity along the axial direction, x, of the packed capillary column (Fig. 3). The results in Fig. 5 clearly show that the value of Pe_{intrap} is greater than unity for all the values of n_T and E_x considered in this work. For a given value of E_x, it can be observed that the behavior of Pe_{intrap} is non-linear when the value of n_T is in the range of 2.0 to 4.5; this is due to the changes occurring in the value of the pore diffusion coefficient, D_p, of the solute (Fig. 4) in this range of values of the pore connectivity, n_T. For values of n_T greater than 4.5, the value of Pe_{intrap} increases only slightly with increasing values of n_T while the increase in the value of Pe_{intrap} is substantial with increasing values of E_x; this occurs because the effect of E_x on the value of $\langle v_{intrap,x} \rangle$ is significantly larger than the effect of n_T on the magnitude of $\langle v_{intrap,x} \rangle$, as the results in Fig. 3 indicate. The values of Pe_{intrap} in Fig. 5b are smaller, for a given value of E_x, than the values of Pe_{intrap} in Fig. 5a because the magnitude of the pore diffusion coefficient, D_p, of lysozyme in the pore network model with coordination number 18 is significantly larger than the value of D_p in the pore network model with coordination number six.

It has been shown [14–17] that there is a departure from spherical symmetry of the isoconcentration profiles of the adsorbate molecules in spherical porous particles when the magnitude of the intraparticle velocity is greater than zero (this implies that the magnitude of the intraparticle Peclet number, Pe_{intrap}, is greater than zero). This spherical asymmetry increases the adsorbate availability in the pore fluid and also increases the concentration of the adsorbate in the adsorbed phase in the upstream half of the spherical porous adsorbent particles; as the value of the intraparticle velocity increases and the adsorbate concentration minimum moves downstream, the overall adsorbate content of the spherical porous adsorbent particles increases, and thus, the dynamic utilization of the adsorptive capacity of the column increases [14–17]. The technique of confocal microscopy [18,19] and the direct measurement method of Gustavsson et al. [20] could represent two possible methods for the experimental detection of intraparticle EOF.

4. Conclusions

The results obtained from the pore network model employed in this work, clearly show that the mag-

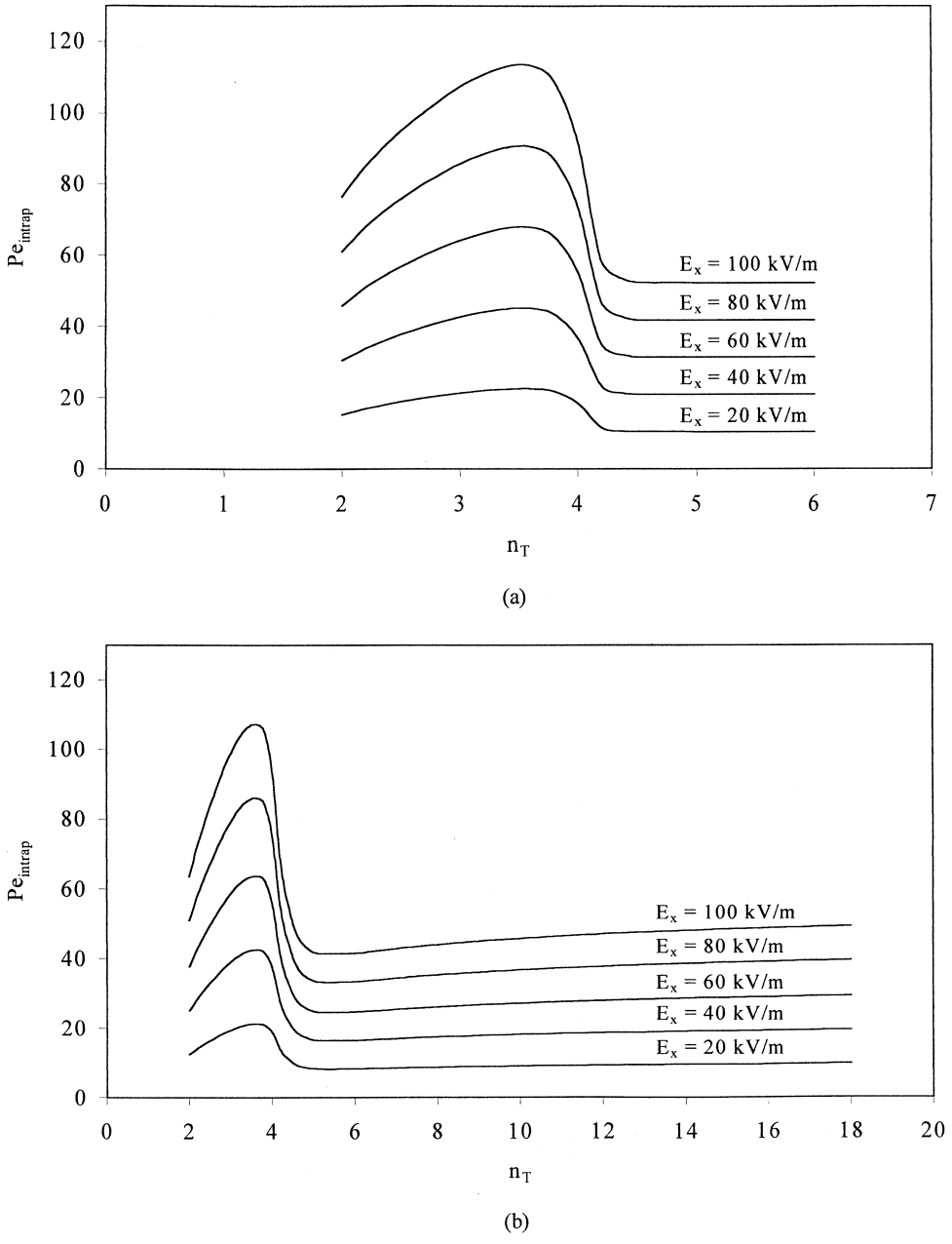

Fig. 5. Intraparticle Peclet number, Pe_{intrap}, versus the intraparticle pore connectivity, n_T, for different values of the applied electric potential difference per unit length, E_x. (a) Pore network model whose coordination number is equal to six. (b) Pore network model whose coordination number is equal to 18.

nitudes of the intraparticle electroosmotic velocity, $\langle v_{intrap,x} \rangle$, and volumetric flow-rate, Q_{intrap}, in the pores of the charged porous silica particles considered in this study are greater than zero. Thus, the intraparticle Peclet number, Pe_{intrap}, of a solute in these charged porous silica particles would be greater than zero, and, in fact, the intraparticle Peclet number, Pe_{intrap}, of lysozyme is greater than unity

for all the values of the intraparticle pore connectivity, n_T, and of the applied electric potential difference per unit length, E_x, considered in this work. Also, the values of the intraparticle electroosmotic velocity, $\langle v_{intrap,x} \rangle$, and volumetric flow-rate, Q_{intrap}, as well as the magnitude of the pore diffusion coefficient, D_p, of the solute increase as the value of the pore connectivity, n_T, of the intraparticle pores increases. The intraparticle EOF mass transfer mechanism can contribute significantly [1,3,4,14–17] in (i) decreasing the intraparticle mass transfer resistance, (ii) decreasing the dispersive mass transfer effects, and (iii) increasing the intraparticle mass transfer rates so that high column efficiency and resolution can be obtained, if the appropriate chemistry is employed in the mobile liquid phase and in the charged porous particles [9–12].

5. Nomenclature

A_{cs} Means Cross-sectional area of the porous medium (porous particle), m^2

C_∞ Means Concentration of symmetric electrolyte, mol/m^3

CEC Means Capillary electrochromatography

D_{mf} Means Free molecular diffusion coefficient of solute, m^2/s

D_p Means Pore diffusion coefficient of solute in the porous particle, m^2/s

d_{intrap} Means Diameter of intraparticle pore, m

d_p Means Particle diameter ($d_p = 2r_p$), m

E_x Means Applied electric potential difference per unit length along the axial direction, x, of the capillary column, kV/m

EOF Means Electroosmotic flow

L Means Lattice size

n_T Means Pore connectivity of the intraparticle pores, dimensionless

Pe_{intrap} Means Intraparticle Peclet number defined in Eq. (2) (see also Eq. (3)), dimensionless

Q_{inters} Means Interstitial volumetric flow-rate due to electroosmotic flow in the interstitial channels (pores) for bulk flow in the capillary column, m^3/s

Q_{intrap} Means Intraparticle volumetric flow-rate due to electroosmotic flow in the pores of the charged porous silica particles packed in the capillary column, m^3/s

Q_{total} Means Total volumetric flow-rate due to electroosmotic flow through the capillary column ($Q_{total} = Q_{inters} + Q_{intrap}$), m^3/s

R Means Radius of capillary column, m

R_{ic} Means Radius of interstitial channel (pore) for bulk flow, m

R_{pore} Means Radius of a pore in the pore network model, m

r_p Means Particle radius ($r_p = d_p/2$), m

T Means temperature, K

t_c Means Convective (intraparticle electroosmotic flow) response time, s

t_d Means Diffusional response time, s

$\langle v_{intrap,x} \rangle$ Means superficial intraparticle velocity of the electroosmotic flow along the axial direction, x, of the capillary column, m/s

x Means Axial direction of the capillary column

Greek letters

α_1 Means Effective molecular radius of solute, m

β Means Hindrance parameter that accounts for steric effects and hindered diffusion, dimensionless

δ Means Fixed charge density on the surface of the charged porous particles and on the surface of the interstitial and intraparticle pores of the network model, C/m^2

ϵ Means Dielectric constant of the liquid solution, $C^2\ N^{-1}\ m^{-2}$

ϵ_b Means Bed porosity in the capillary column, dimensionless

ϵ_p Means Porosity of the charged porous particle, dimensionless

ζ_p Means Zeta potential at the particle surface, V

λ Means Debye length (characteristic thickness of double layer), m

μ Means Mean diameter of the intraparticle pores, m

σ Means Standard deviation of the diameter of the intraparticle pores, m

τ Means Tortuosity factor, dimensionless

Acknowledgements

The authors gratefully acknowledge support of this work by Criofarma and the Biochemical Processing Institute of the University of Missouri-Rolla.

References

[1] A.I. Liapis, B.A. Grimes, J. Chromatogr. A 877 (2000) 181.
[2] A.S. Rathore, Cs. Horváth, J. Chromatogr. A 781 (1997) 185.
[3] J.J. Meyers, A.I. Liapis, J. Chromatogr. A 827 (1998) 197.
[4] J.J. Meyers, A.I. Liapis, J. Chromatogr. A 852 (1999) 3.
[5] A.I. Liapis, J.J. Meyers, O.K. Crosser, J. Chromatogr. A 865 (1999) 13.
[6] D. Stauffer, A. Aharony, Introduction to Percolation Theory, 2nd Edition, Taylor and Francis, London, 1992.
[7] R.F. Probstein, Physicochemical Hydrodynamics, Butterworth, Stoneham, MA, 1989.
[8] W.B. Russel, D.A. Saville, W.R. Schowalter, Colloidal Dispersions, Cambridge University Press, Cambridge, 1989.
[9] J. Ståhlberg, Anal. Chem. 69 (1997) 3812.
[10] R. Asiaie, X. Huang, D. Farnan, Cs. Horváth, J. Chromatogr. A 806 (1998) 251.
[11] K. Walhagen, K.K. Unger, A.M. Olsson, M.T.W. Hearn, J. Chromatogr. A 853 (1999) 263.
[12] S. Lüdtke, Ph.D. Dissertation, Institut für Anorganische Chemie und Analytische Chemie, Johannes Gutenberg-Universität, Mainz, 1999.
[13] H. Sober (Ed.), Handbook of Biochemistry: Selected Data for Molecular Biology, Chemical Rubber Company, Cleveland, OH, 1968.
[14] A.I. Liapis, Y. Xu, O.K. Crosser, A. Tongta, J. Chromatogr. A 702 (1995) 45.
[15] G.A. Heeter, A.I. Liapis, J. Chromatogr. A 711 (1995) 3.
[16] Y. Xu, A.I. Liapis, J. Chromatogr. A 724 (1996) 13.
[17] G.A. Heeter, A.I. Liapis, J. Chromatogr. A 734 (1996) 105.
[18] A. Ljunglöf, J. Thömmes, J. Chromatogr. A 813 (1998) 387.
[19] A. Ljunglöf, P. Bergvall, R. Bhikhabhai, R. Hjorth, J. Chromatogr. A 844 (1999) 129.
[20] P.-E. Gustavsson, A. Axelsson, P.-O. Larsson, J. Chromatogr. A 795 (1998) 199.